Stabilization of Hypophosphite in the Binding Pocket of a Dinuclear Macrocyclic Complex: Synthesis, Structure, and Properties of [Ni₂L(μ-O₂PH₂)]BPh₄ (L = N₆S₂ Donor Ligand)

Jochen Lach,[†] Alexander Jeremies,[†] Vasile Lozan,[†,§] Claudia Loose,[‡] Torsten Hahn,[‡] Jens Kortus,[‡] and Berthold Kersting*[,†]

[†]Institut für Anorganische Chemie, Universität Leipzig, Johannisallee 29, D-04103 Leipzig, Germany
[‡]Institut für Theoretische Physik, TU Bergakademie Freiberg, Leipziger Str. 23, 09596 Freiberg

S *Supporting Information*

ABSTRACT: The dinickel(II) complex $[Ni_2L(ClO_4)]ClO_4$ (**1**), where L^{2-} represents a 24-membered macrocyclic hexaamine-dithiophenolate ligand, reacts with $[nBu_4N]H_2PO_2$ to form the hypophosphito-bridged complex $[Ni_2L(\mu\text{-}O_2PH_2)]^+$, which can be isolated as an air-stable perchlorate $[Ni_2L(\mu\text{-}O_2PH_2)]ClO_4$ (**2**) or tetraphenylborate $[Ni_2L(\mu\text{-}O_2PH_2)]BPh_4$ (**3**) salt. **3**·MeCN crystallizes in the triclinic space group $P\bar{1}$. The bisoctahedral $[Ni_2L(\mu\text{-}O_2PH_2)]^+$ cation has a $N_3Ni(\mu_{1,3}\text{-}O_2PH_2)(\mu\text{-}S)_2NiN_3$ core structure with the hypophosphito ligand attached to the two Ni^{II} ions in a $\mu_{1,3}$-bridging mode. The hypophosphito ligand is readily replaced by carboxylates, in agreement with a higher affinity of the $[Ni_2L]^{2+}$ dication for more basic oxoanions. Treatment of $[Ni_2L(\mu\text{-}O_2PH_2)]ClO_4$ with H_2O_2 or MCPBA results in the oxidation of the bridging thiolato to sulfonato groups. The hypophosphito group is not oxidized under these conditions due to the steric protection offered by the supporting ligand. An analysis of the temperature-dependent magnetic susceptibility data for **3** reveals the presence of ferromagnetic exchange interactions between the Ni^{II} ($S = 1$) ions with a value for the magnetic exchange coupling constant J of +22 cm^{-1} ($\mathbf{H} = -2J\mathbf{S_1S_2}$). These results are additionally supported by DFT (density functional theory) calculations.
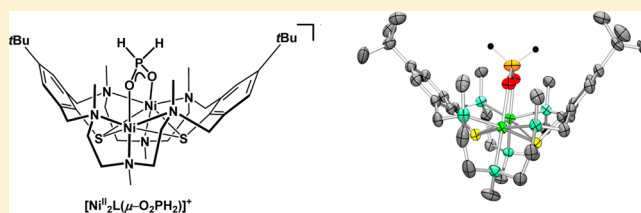
INTRODUCTION

Several complexes containing the hypophosphite ion $(H_2PO_2^-)$ as a ligand have been reported and crystallographically characterized. These include structures of d-block,[1–3] s-block,[4] p-block,[5] lanthanide,[6,7] and actinide metals.[8] The hypophosphito ligand in these metal complexes is very flexible in its coordination (Figure 1). The doubly bridging μ_2,[5,8,9]
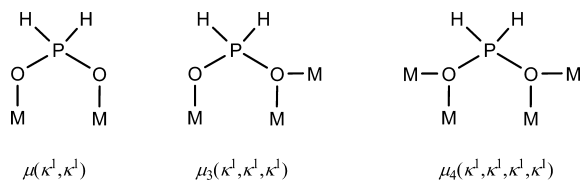

Figure 1. Coordination modes of the hypophosphito ligand.

triply bridging μ_3,[1,3] and quadruply bridging μ_4 modes[2,4] are all represented. The behavior of the $H_2PO_2^-$ ion in these compounds is expected to be interesting due to its redox behavior. In fact, the hypophosphite is sensitive toward oxidizing agents, and oxidation to phosphite (HPO_3^{2-}) or phosphate (PO_4^{3-}) has been reported in several cases.[7,10,11]

Recently, we have been exploring the chemistry of bisoctahedral transition metal complexes of the type $[M_2L(L')]^{n+}$ where L^{2-} represents a supporting macrocycle with an N_6S_2 donor set and L' is a main group or transition metal oxoanion. The X-ray crystal structures of the following complexes have been reported: $[Ni_2L(\mu\text{-}PO_2(OH)_2)]BPh_4$,[12] $[Ni_2L(\mu\text{-}SO_4)]$,[13] $[Ni_2L(\mu\text{-}ClO_4)]BPh_4$, $[Co_2L(\mu\text{-}MoO_4)]$,[14] $[Ni_2L(\mu\text{-}CrO_4)]$,[13] $[Ni_2L(\mu\text{-}MoO_4)]$,[13] $[Co_2L(\mu\text{-}MoO_2(OH)\text{-}(OMe))]^+$,[14] $[Ni_2L(\mu\text{-}PO_2(OC_6H_4\text{-}pNO_2)_2)]^+$,[15] and $[Ni_2L(\mu\text{-}VO_2(OMe)_2)]^+$.[16] The oxo- and oxo-alkoxo anions are all coordinated in a $\mu_{1,3}$-bridging $O_2E(OR)_2$ mode thereby generating $M_2(\mu\text{-}O_2E(=O)_2)$, $M_2(\mu\text{-}O_2E(\text{-}OR)_2)$, or $M_2(\mu\text{-}O_2E(=O)(OR))$ structures with two oxo, hydroxido (R = H), or alkoxo (R = alkyl) groups, respectively, which are deeply buried in the pocket provided by the supporting ligand.

To further develop the coordination chemistry of these complexes, we decided to prepare and characterize a $[Ni_2L(\mu\text{-}L')]^+$ complex bearing a $H_2PO_2^-$ ion as a coligand. The motivation for this work is as follows. First, nickel(II) hypophosphito complexes are not very stable, a behavior which is taken advantage of in electroless nickel plating.[17,18] Second, there exists only little information in the literature regarding the bonding of a $H_2PO_2^-$ ion in dinuclear nickel(II) complexes. Third, incorporation of the $H_2PO_2^-$ ion in the binding pocket of the $[Ni_2L]^{2+}$ complex might lead to an alteration of its reactivity. Finally, the type and magnitude of

magnetic coupling via a $H_2PO_2^-$ unit is scarce. Herein, we report on the successful preparation and isolation of the complex salts **2** and **3** containing the hypophosphito-bridged dinickel(II) complex cation $[Ni_2L(\mu\text{-}O_2PH_2)]^+$ (Figure 2). The crystal structure, electrochemistry, reactivity features, magnetic properties, and DFT calculations of **3** are also described.
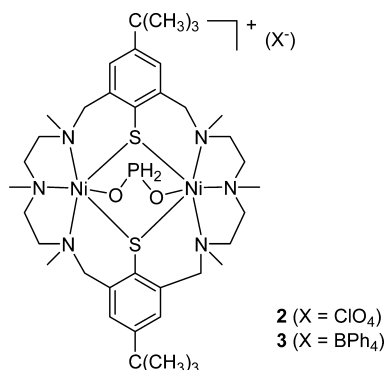

Figure 2. Chemical structure of the $[Ni_2L(\mu\text{-}O_2PH_2)]^+$ complex in the salts **2** and **3**.

EXPERIMENTAL SECTION

General. Unless otherwise noted the preparations were carried out under an argon atmosphere by using standard Schlenk techniques. The complex salt $[Ni_2L(\mu\text{-}ClO_4)]ClO_4$ (**1**) was prepared as described in the literature.[13] Melting points were determined in capillaries and are uncorrected. The infrared spectra were recorded as KBr discs using a Bruker Tensor 27 FT-IR-spectrophotometer. Electronic absorption spectra were recorded on a Jasco V-670 UV–vis–NIR spectrophotometer. Elemental analysis were carried out on a VARIO EL elemental analyzer. ESI mass spectra were recorded on a Bruker Daltronics ESQUIRE3000 PLUS spectrometer. Cyclic voltammetry measurements were carried out at 25 °C with an EG&G Princeton Applied Research potentiostat/galvanostat model 263 A. The cell contained a Pt working electrode, a Pt wire auxiliary electrode, and a Ag wire as reference electrode. Concentrations of solutions were 0.10 M in supporting electrolyte ($[n\text{-}Bu_4N]PF_6$) and ca. 1×10^{-3} M in sample. Cobaltocene was used as internal standard.[19] All potentials were converted to the SCE reference. Temperature-dependent magnetic susceptibility measurements on powdered solid samples of compound **3** were carried out to study the magnetic exchange interactions in the dinuclear Ni^{II} complex. The susceptibility data of **3** were measured between 2 and 330 K using a MPMS 7XL SQUID magnetometer (Quantum Design) in an applied external magnetic field of 0.5 T.

Caution! Perchlorate salts of transition metal complexes are hazardous and may explode. Only small quantities should be prepared and great care should be taken.
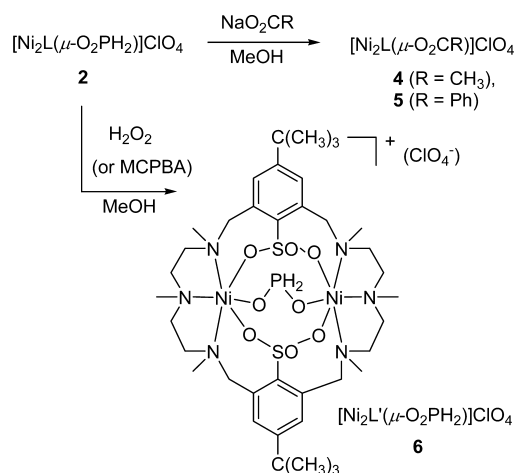
$[Ni_2L(\mu\text{-}O_2PH_2)]ClO_4$ (2). To a solution of **1** (92 mg, 0.10 mmol) in methanol (30 mL) was added with stirring a solution of $(nBu_4N)\text{-}H_2PO_2$ (82.5 mg, 0.268 mmol) in methanol (5 mL) at room temperature. The reaction mixture was stirred for about 4 h after which time solid $LiClO_4\cdot 3H_2O$ (160 mg, 1.00 mmol) was added. The solution was concentrated under reduced pressure until bright green crystals formed, which were filtered, washed with cold methanol, and dried in air. The crude product was purified by recrystallization from a mixed acetonitrile/ethanol solution. Yield: 73 mg (77%). UV–vis (CH_3CN): λ_{max}/nm (ε/M^{-1} cm^{-1}) = 671 (24), 1134 (73). Mp 312–314 °C (decomp). IR (KBr, cm^{-1}): $\tilde{\nu}$ = 3439 (m), 3042 (w), 2993 (w), 2957 (s), 2900 (m), 2868 (s), 2806 (w), 2780 (w), 2332 (m) [$\nu_s(PH_2)$], 2298 (m) [$\nu_{as}(PH_2)$], 2273 (w), 2163 (w), 1618 (w), 1603 (vw), 1527 (w), 1482 (w), 1461 (s), 1422 (w), 1393 (w), 1363 (m), 1349 (w), 1323 (w), 1307 (m), 1264 (m), 1232 (w), 1195 (s) [$\nu_{as}(PO_2)$], 1169 (w), 1156 (w), 1098 (vs), 1087 (vs), 1076 (vs),

[$\nu_3(ClO_4^-)$], 1041 (m) [$\nu_{symm}(PO_2)$], 1002 (s), 981 (w), 928 (w), 912 (w), 882 (w), 826 (s), 817 (w), 810 (s), 751 (w), 625 (s) [$\nu_4(ClO_4^-)$], 563 (w), 535 (w), 483 (m), 442 (w), 434 (w), 425 (w), 416 (w). Electrospray ionization mass spectrometry (ESI(+)-MS): m/z (CH_3CN) = 849.3 $[M]^+$. Anal. Calcd for $C_{38}H_{66}ClN_6Ni_2O_6PS_2$ (950.91): C 48.00, H 7.00, N 8.84, S 6.74. Found: C 47.88, H 7.14, N 8.74, S 6.63. Cyclic voltammetry (CH_3CN): E/V (ΔE_p/ V) vs SCE: 0.50 V (0.09 V), 1.24 V (0.12 V).

$[Ni_2L(\mu\text{-}O_2PH_2)]BPh_4$ (3). A solution of $NaBPh_4$ (342 mg, 1.00 mmol) in methanol (2 mL) was added to a solution of **2** (95 mg, 0.10 mmol) in methanol (40 mL) and stirred for 1 h. The resulting bright green precipitate was filtered, washed with methanol, and dried in air to give 107 mg (91%) of **3** as a green, air-stable, microcrystalline powder. Mp 319–320 °C (decomp.). UV–vis (CH_3CN): λ_{max}/nm (ε/ M^{-1} cm^{-1}) = 304 (9679), 666 (20), 1133 (53). IR (KBr, cm^{-1}): $\tilde{\nu}$ = 3159 (vw), 3124 (vw), 3053 (s), 3041 (sh), 3030 (sh), 3013 (sh), 2999 (m), 2982 (w), 2962 (s), 2934 (w), 2900 (m), 2873 (s), 2334 (s), 2300 (m), 2272 (w), 1946 (m), 1881 (m), 1820 (m), 1761 (w), 1707 (m), 1625 (m), 1581 (m), 1562 (w), 1478 (vs), 1459 (s), 1426 (s), 1382 (m), 1362 (w), 1349 (vw), 1324 (vw), 1305 (m), 1265 (m), 1232 (w), 1191 (s, br), 1171 (vw), 1152 (s), 1130 (vw), 1107 (vw), 1086 (m), 1075 (s), 1067 (m), 1058 (sh), 1039 (sh), 1033 (s), 1001 (m), 979 (m), 927 (w), 910 (w), 881 (s), 861 (w), 847 (m), 824 (m), 809 (s), 741 (w), 733 (s), 706 (vs), 625 (w), 610 (m), 563 (m), 540 (w), 532 (vw), 481 (w), 467 (w), 416 (w). Electrospray ionization mass spectrometry (ESI(+)-MS): m/z (CH_3CN) = 849.3 $[M]^+$. Single crystals of **3**·MeCN suitable for an X-ray structure analysis were grown by slow evaporation of an ethanol/acetonitrile solution of **3**. These crystals slowly lose solvent molecules of solvent of crystallization at ambient temperature and turn dull. Anal. Calcd (%) for $C_{62}H_{86}BN_6Ni_2O_2PS_2\cdot 3H_2O$ (1170.69 + 54.05): C 60.80, H 7.57, N 6.86, S 5.24. Found: C 60.70, H 7.28, N 6.81, S 5.37.

The complexes **4** and **5** below have been reported previously, but were obtained here in another fashion, by substitution of the hypophosphito coligand in **2** (see Scheme 1). The earlier method used the chloro-bridged complex $[Ni_2L(\mu\text{-}Cl)]ClO_4$ as starting material.[12,20]

Scheme 1. Carboxylate Exchange and S-Oxygenation Reactions of Compound 2

$[Ni_2L(\mu\text{-}O_2CCH_3)]ClO_4$ (4). To a solution of **2** (95 mg, 0.10 mmol) in methanol (30 mL) was added with stirring a solution of sodium acetate (82 mg, 1.00 mmol) in methanol (10 mL) at room temperature. The reaction mixture was stirred for about 24 h after which time solid $LiClO_4\cdot 3H_2O$ (160 mg, 1.00 mmol) was added. The solution was concentrated under reduced pressure until bright green crystals formed, which were filtered, washed with cold methanol, and dried in air. The crude product was purified by recrystallization from a mixed acetonitrile/ethanol solution. Yield: 79 mg (83%). IR (KBr, cm^{-1}): $\tilde{\nu}$ = 3442 (m), 2962 (m), 2870 (m), 2802 (w), 1589 (s,

$\nu_{as}(RCO_2^-))$, 1459 (s), 1427 (m, $\nu_s(RCO_2^-)$), 1396 (w), 1363 (w), 1308 (w), 1266 (w), 1233 (w), 1202 (w), 1170 (w), 1153 (w), 1097 (s), 1080 (s), 1058 (m), 1039 (m), 1002 (w), 983 (w), 931 (w), 912 (w), 890 (w), 880 (w), 826 (m), 817 (w), 807 (w), 752 (w), 662 (w), 624 (m), 564 (w), 534 (w), 492 (w), 417 (w). Electrospray ionization mass spectrometry (ESI(+)-MS): m/z (CH$_3$CN) = 843.2 [M]$^+$. UV−vis (MeCN): λ_{max}/nm (ε/M^{-1} cm^{-1}) = 650 (26), 1131 (67). These data are identical with those reported in the literature.[12]

[Ni$_2$L(μ-O$_2$CPh)]ClO$_4$ (5). To a solution of **2** (95 mg, 0.10 mmol) in methanol (30 mL) was added with stirring a solution of sodium benzoate (144 mg, 1.00 mmol) in methanol (10 mL) at room temperature. The reaction mixture was stirred for about 24 h after which time solid LiClO$_4$·3H$_2$O (160 mg, 1.00 mmol) was added. The solution was concentrated under reduced pressure until bright green crystals formed, which were filtered, washed with cold methanol, and dried in air. The crude product was purified by recrystallization from a mixed acetonitrile/ethanol solution. Yield: 75 mg (79%). IR (KBr, cm^{-1}): $\tilde{\nu}$ = 3445 (m), 2965 (m), 2897 (m), 2868 (m), 2806 (w), 1600 (m), 1586 (m), 1569 (s), 1463 (s), 1428 (s), 1406 (m), 1363 (m), 1308 (w), 1263 (w), 1232 (w), 1202 (w), 1172 (w), 1153 (w), 1096 (s), 1057 (m), 1040 (m), 1001 (w), 982 (w), 931 (w), 913 (w), 882 (w), 826 (m), 753 (w), 708 (w), 675 (w), 623 (m), 564 (w), 538 (w), 493 (w), 471 (w), 443 (w), 418 (w). Electrospray ionization mass spectrometry (ESI(+)-MS): m/z (CH$_3$CN) = 905.3 [M]$^+$. UV−vis (MeCN): λ_{max}/nm (ε/M^{-1} cm^{-1}) = 651 (29), 1123 (69). These data are identical with those reported in the literature.[20]

[Ni$_2$L′(μ-O$_2$PH$_2$)]ClO$_4$ (6), Where L′ is the Oxidized Hexaza-(disulfonato) Form of (L)$^{2-}$ (see Scheme 1). Method A (Oxidation with Hydrogen Peroxide). To a solution of **2** (95 mg, 0.10 mmol) in methanol (30 mL) was added with stirring an excess of hydrogen peroxide (0.28 mL, 50 wt % solution in water, 5.00 mmol) at room temperature. The reaction mixture was stirred for about 7 d after which time solid LiClO$_4$·3H$_2$O (160 mg, 1.00 mmol) was added. The solution was concentrated under reduced pressure until pale-green crystals formed, which were filtered, washed with cold methanol, and dried in air. The crude product was purified by recrystallization from a mixed acetonitrile/ethanol solution. Yield: 75 mg (71%). IR (KBr, cm^{-1}): $\tilde{\nu}$ = 3449 (m), 2967 (m), 2909 (w), 2873 (m), 2370 (w), 2355 (w), 2338 (m), 2313 (m), 1618 (w), 1599 (w), 1561 (w), 1482 (m), 1410 (w), 1397 (w), 1382 (w), 1362 (w), 1301 (w), 1237 (s), 1168 (m), 1090 (s), 1032 (m), 999 (w), 974 (w), 918 (w), 899 (m), 831 (m), 818 (m), 751 (w), 706 (m), 670 (m), 638 (m), 623 (m), 592 (w), 559 (w), 543 (w), 492 (w), 459 (w). Electrospray ionization mass spectrometry (ESI(+)-MS): m/z (CH$_3$CN) = 945.1 [M]$^+$. UV−vis (MeCN): λ_{max}/nm (ε/M^{-1} cm^{-1}) = 403 (62), 460 (20), 690 (18), 1174 (19). Anal. Calcd for C$_{38}$H$_{66}$ClN$_6$Ni$_2$O$_{12}$PS$_2$ (1046.91): C 43.60, H 6.35, N 8.03, S 6.13. Found: C 43.97, H 6.34, N 7.78, S 6.27.

Method B (Oxidation with meta-Chloroperoxybenzoic Acid, mCPBA). To a solution of **2** (95 mg, 0.10 mmol) in dichloromethane (40 mL) was added with stirring *meta*-chloroperbenzoic acid (432 mg, 2.50 mmol) at room temperature. The reaction mixture was stirred for about 24 h after which time solid LiClO$_4$·3H$_2$O (160 mg, 1.00 mmol) was added. The solution was concentrated under reduced pressure to produce pale-green crystals, which were filtered, washed with cold methanol, and dried in air. The crude product was purified by recrystallization from a mixed acetonitrile/ethanol solution. Yield: 70 mg (67%). The analytical data of this material are identical to those of compound **6** prepared by method A.

Spectroscopic Titration. For the UV−vis−NIR experiments a 4.00×10^{-3} M solution of **2** in MeCN/MeOH (4:1) was aliquoted into nine samples (0.8 mL) to which increasing equivalents of a 2.56×10^{-2} M sodium acetate solution were added using an Eppendorf buret. In that manner solutions containing 0−2 equiv of NaOAc were obtained and allowed to react for 5 h prior measuring. Spectra were recorded on a Jasco V-670 UV−vis−NIR spectrophotometer in the range from 1600 to 190 nm. All spectra were corrected for dilution and expressed as molar extinction coefficient versus wavelength.

Crystallography. A suitable crystal of compound **3**·MeCN was selected and mounted on the tip of a glass fiber. The intensity data were collected on a Bruker Smart CCD diffractometer using SMART.[21] Data processing was accomplished with SAINT.[22] An empirical absorption correction was performed with the program SADABS.[23] The structure was solved by direct methods in SHELXS[24] and refined by full-matrix least-squares on F^2 using SHELXTL (version 5.1).[25] All non-hydrogen atoms were refined with anisotropic displacement parameters. The hydrogen atoms were placed at calculated positions, using appropriate riding or rotation models (HFIX 23 for CH$_2$, HFIX 43 for aromatic CH, and HFIX 133 for CH$_3$), and assigned isotropic thermal parameters (e.g., U_{iso}(H) = 1.2 × U_{iso}(parent) or U_{iso}(H) = 1.5 × U_{iso}(C) for methyl groups). The hydrogen atoms of the hypophosphite were placed at ideal positions assuming a P−H distance of 1.40 Å and a tetrahedral geometry and were given isotropic thermal parameters 1.2 times the thermal parameter of the phosphorus atom. Both *tert*-butyl groups of the supporting ligand were found to be rotationally disordered. A split atom model with restrained C−C and C···C distances was applied using SADI instructions implemented in SHELXTL. The site occupancies of the two positions were refined as follows: C(32a)−C(33a) /C(32b)−C(34b): 0.71(1)/0.29(1), and C(36a)−C(38a) /C(36b)−C(38b): 0.56(1)/0.44(1). Graphics were obtained with ORTEP 3 for Windows.[26]

Crystallographic data for **3**·MeCN: C$_{64}$H$_{89}$BN$_7$Ni$_2$O$_2$PS$_2$ (1211.74 g mol^{-1}), triclinic, space group $P\bar{1}$, a = 13.179(3) Å, b = 15.736(3) Å, c = 16.799(3) Å, α = 108.48(3)°, β = 91.90(3)°, γ = 107.61(3)°, V = 3117.1(11) Å^3, Z = 2, ρ = 1.291 g cm^{-3}, μ(Mo Kα) = 0.745 mm^{-1}, crystal size 0.18 × 0.15 × 0.10 mm^3, θ limits 1.29−28.35°. Of 28 567 measured reflections (R_{int} = 0.0399), 14 655 were unique and 7874 observed ($I > 2\sigma I$). Final residuals: R1 = 0.0401, wR2 = 0.0829 (for observed data), R1 = 0.0987, wR2 = 0.1234 for all data. Max, min peaks: 0.418, −0.620 e/Å^3. CCDC-870563 contains the supplementary crystallographic data for this paper. These data can be obtained free of charge from The Cambridge Crystallographic Data Centre via www.ccdc.cam.ac.uk/data_request/cif.
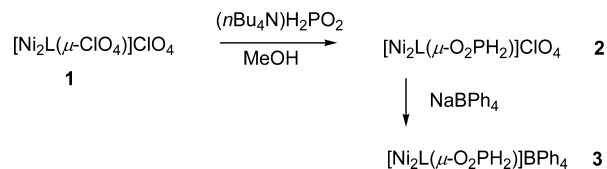
Electronic Structure Calculations. The density functional calculations of the free, isolated [Ni$_2$L(μ-O$_2$PH$_2$)]$^+$ cation (in **3**) have been carried out using the Naval Research Laboratory Molecular Orbital Library (NRLMOL) program package. NRLMOL is an all-electron implementation of DFT including large Gaussian orbital basis sets, numerically precise variational integration and an analytic solution of Poisson's equation in order to accurately determine the self-consistent potentials, secular matrix, total energies, and Hellmann−Feynman−Pulay forces.[27−34] The calculations have been carried out using the generalized gradient approximation of Perdew, Burke, and Enzerhof (PBE) for the exchange and correlation functional.[35,36] For comparison we carried out calculations using the ORCA[37,38] program package (revision 2.80) including the B3LYP[39] functional and Ahlrichs triple-ζ valence basis set.[40] Starting from the experimental X-ray structure we generated a molecular model of the isolated complex cation which has been used for the calculation. The magnetic exchange coupling itself was obtained by mapping the energy difference between the high-spin (S = 2) and a low-spin (S = 0) configuration of the molecule to the **H** = $-2J$**S$_1$S$_2$** Heisenberg Hamiltonian. The low-spin configuration was obtained using the broken symmetry approach detailed previously.[41]

■ RESULTS AND DISCUSSION

Synthesis and Spectroscopic Characterization. The substitution reaction of [Ni$_2$L(μ-ClO$_4$)]ClO$_4$ (**1**)[13] with [*n*-Bu$_4$N]H$_2$PO$_2$ in methanol results in the smooth formation of the hypophosphito complex [Ni$_2$L(μ-O$_2$PH$_2$)]$^+$, isolable as a pale-green, microcrystalline perchlorate salt **2** in good yields (Scheme 2). Complex salt **2** is readily soluble in organic solvents such as methanol, acetonitrile, and DMF, but virtually insoluble in water. The corresponding tetraphenylborate salt [Ni$_2$L(μ-O$_2$PH$_2$)]BPh$_4$ (**3**) is accessible by salt metathesis of **2** with NaBPh$_4$ in methanol.

Compounds **2** and **3** are thermally stable up to 100 °C in air in solution (ethylene glycol) as well as in the solid state. This

Scheme 2. Synthesis of Compounds 2 and 3

$$[Ni_2L(\mu\text{-}ClO_4)]ClO_4 \quad \xrightarrow[\text{MeOH}]{(nBu_4N)H_2PO_2} \quad [Ni_2L(\mu\text{-}O_2PH_2)]ClO_4 \quad \mathbf{2}$$

1

$$\downarrow \quad NaBPh_4$$

$$[Ni_2L(\mu\text{-}O_2PH_2)]BPh_4 \quad \mathbf{3}$$

stability is quite remarkable given that nickel(II) is readily reduced by hypophosphite. Moreover, hypophosphito complexes are also very prone to oxidation by air oxygen.[7] The stabilization can be attributed to encapsulation in a molecular pocket, which has precedence in the literature. Fujita, for example, has reported on the stabilization of a cyclic trisilanol in the pocket of a coordination cage.[42]

All new compounds gave satisfactory elemental analysis and were further characterized by ESI mass spectrometry, IR, and UV−vis spectroscopy. The electrospray ionization mass spectrum (ESI(+)-MS) of a dilute acetonitrile solution of **2** displays a molecular ion peak at m/z = 849.3 in good agreement with the formulation of the $[Ni_2L(\mu\text{-}O_2PH_2)]^+$ cation. Infrared data for **2** and **3** and their assignments are listed in Table 1. IR data for $[n\text{-}Bu_4N]H_2PO_2$ are included for comparison.

Table 1. Selected IR/cm^{-1} and UV−vis/nm spectral data for 2 and 3^a

	$\nu_s(PH_2)$	$\nu_{as}(PH_2)$	$\nu_{as}(PO_2)$	$\nu_s(PO_2)/$	ν_1	ν_2
$[nBu_4N]$ H_2PO_2	2345	2308	1198	1052		
2	2332 m	2298 m	1195 m	1041 m	1134	671
3	2334 s	2300 m	1191 s,br	1039 sh	1133	666

^{a}m = medium, s = strong, br = broad, sh = shoulder.

The IR spectra show bands arising from the $[Ni_2L]^{2+}$ fragments, the ClO_4^- or BPh_4^- counterions, and the $H_2PO_2^-$ groups. Complex salt **2** gives rise to two νPH bands, as in other $H_2PO_2^-$ complexes,[43] at 2332 and 2298 cm^{-1}, which can be assigned to the symmetric and antisymmetric νPH_2 stretching modes, respectively. The two intense bands at 1195 and 1041 cm^{-1}, on the other hand, can be attributed to the antisymmetric and symmetric νPO_2 stretching modes.[44] The IR spectrum of **3** is very similar to that of **2**, and the frequencies of corresponding $H_2PO_2^-$ vibrations are identical (within experimental error). Note that the IR absorptions of the coordinated $H_2PO_2^-$ moieties in **2** and **3** are shifted by as much as 13 cm^{-1} relative to the corresponding values of the free $H_2PO_2^-$ ion.[45] This frequency shift is in good agreement with coordination of the $H_2PO_2^-$ group.

The electronic absorption spectrum for an acetonitrile solution of **2** in the 300−1600 nm region reveals two weak absorption bands at 671 and 1134 nm attributable to spin-allowed d−d-transitions of a six-coordinate nickel(II) ion (assigned as $^3A_{2g} \rightarrow {}^3T_{1g}$, $^3A_{2g} \rightarrow {}^3T_{2g}$ in pure octahedral symmetry).[46,47] For **3**, similar absorptions are seen at 666 and 1133 nm. The $^3A_{1g} \rightarrow {}^3T_{1g}(P)$ transition expected for an octahedral Ni^{II} complex is obscured in both cases by strong $RS^- \rightarrow Ni^{II}$ charge transfer transitions below 450 nm.

The ν_1 transition at λ_{max} = 1134 allows us to estimate an octahedral splitting parameter Δ_o of ~8818 cm^{-1} in $[Ni_2L(\mu\text{-}O_2PH_2)]^+$.[48] This value should be compared to a similar but little smaller value Δ_o = 8795 cm^{-1} for the dihydrogenphos-

phato complex $[Ni_2L(\mu\text{-}O_2P(OH)_2)]^+$.[12] It is interesting to note in this respect that a relationship exists between the basicity of the coligand and the ligand field parameter Δ_o in dinuclear nickel(II) complexes supported by the hexamine dithiophenolate macrocycle L^{2-}.[49] For these complexes Δ_o decreases with increasing basicity of the coligands. The present finding that the Δ_o value for the hypophosphito complex which carries the less basic coligand (pK_b ($H_2PO_2^-$) = 12.77) is larger than for the dihydrogenphosphato complex (pK_b ($H_2PO_4^-$) = 11.84) is in excellent agreement with the reported trend.

Cyclic Voltammetry. In order to investigate the redox-behavior of the $[Ni_2L(\mu\text{-}O_2PH_2)]^+$ complex, cyclic voltammetry experiments were carried out. Figure 3 shows the cyclic voltammogram of a 10^{-3} molar acetonitrile solution of the perchlorate salt **2**.
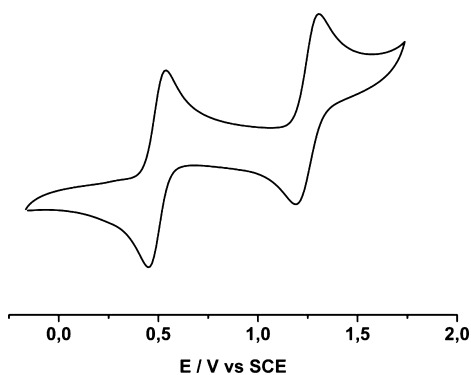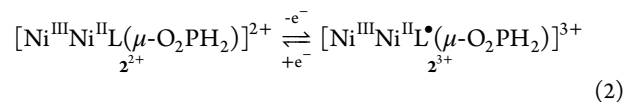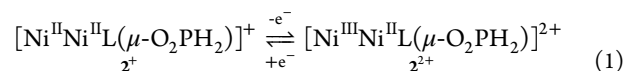
Figure 3. Cyclic voltammogram of **2** in CH$_3$CN at 298 K. Experimental conditions: 0.1 M $[n\text{-}Bu_4N]PF_6$, ca. 1 × 10^{-3} M sample concentration, Pt disk working electrode, Ag wire reference electrode, scan rate 100 mV/s, $[Co(Cp_2)]PF_6$ internal reference.

Two waves, one at $E^1_{1/2}$ = +0.50 V versus SCE with a peak-to-peak separation ΔE_p of 0.09 V and one at $E^2_{1/2}$ = +1.24 V with ΔE_p = 0.12 V, are observed. Coulometric studies reveal that the first oxidation is a one-electron processes. Controlled-potential coulometry of $[Ni_2L(\mu\text{-}O_2PH_2)]ClO_4$ at an applied potential of +1.0 V versus SCE in CH$_3$CN solution at 273 K consumed n = 0.97 e$^-$/complex, while re-reduction at 0 V versus SCE caused transfer of 96% of the charge passed in oxidation. Furthermore, the CV of the electrogenerated $[Ni_2L(\mu\text{-}O_2PH_2)]^{2+}$ dication **2^{2+}** is identical to that of the starting material.[50] The electrochemical properties of $[Ni_2L(\mu\text{-}O_2PH_2)]^+$ are comparable to those of the acetato-bridged complex $[Ni_2L(\mu\text{-}O_2CMe)]^+$ which shows two corresponding waves at $E^1_{1/2}$ = 0.56 V and $E^2_{1/2}$ = 1.36 V.[51] The redox waves can be assigned to metal-centered (Ni^{II}Ni^{II} → Ni^{II}Ni^{III}) and ligand-based oxidations (RS$^-$(thiolate) → RS$^\bullet$ (thiyl radical)) within the $[Ni_2L]^{2+}$ unit as represented in eqs 1 and 2.[51]

In the chosen potential window ranging from −2.0 to +2.5 V versus SCE no redox waves are observed that can be attributed to oxidation or reduction of the O$_2$PH$_2^-$ group. It can be said that the O$_2$PH$_2^-$ unit is redox inactive in this potential range.

$$[Ni^{II}Ni^{II}L(\mu\text{-}O_2PH_2)]^+ \underset{+e^-}{\overset{-e^-}{\rightleftharpoons}} [Ni^{III}Ni^{II}L(\mu\text{-}O_2PH_2)]^{2+}$$
$$\mathbf{2^+} \qquad\qquad\qquad \mathbf{2^{2+}} \qquad (1)$$

$$[Ni^{III}Ni^{II}L(\mu\text{-}O_2PH_2)]^{2+} \underset{+e^-}{\overset{-e^-}{\rightleftharpoons}} [Ni^{III}Ni^{II}L^\bullet(\mu\text{-}O_2PH_2)]^{3+}$$
$$\mathbf{2^{2+}} \qquad\qquad\qquad \mathbf{2^{3+}} \qquad (2)$$

Description of the Crystal Structure of 3·MeCN. An X-ray crystallographic analysis using crystals of 3●MeCN grown from ethanol/acetonitrile was undertaken to unambiguously characterize the complex. 3●MeCN crystallizes triclinic, space group $P\bar{1}$. The crystal structure consists of discrete $[Ni_2L(\mu\text{-}O_2PH_2)]^+$ cations, BPh_4^- anions, and MeCN solvate molecules. Figure 4 provides a perspective view of the molecular structure
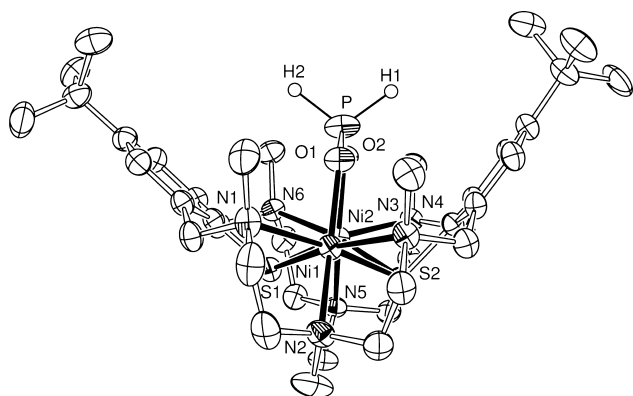

Figure 4. Molecular structure of the $[Ni_2L(\mu\text{-}O_2PH_2)]^+$ cation in crystals of 3●MeCN. Thermal ellipsoids are drawn at the 50% probability level. Hydrogen atoms (except for the PH_2 group) are omitted for clarity. Selected bond lengths/Å and angles/deg: Ni(1)−O(1) 2.026(2), Ni(1)−N(1) 2.224(3), Ni(1)−N(2) 2.150(3), Ni(1)−N(3) 2.257(3), Ni(1)−S(1) 2.444(1), Ni(1)−S(2) 2.521(1), Ni(2)−O(2) 2.034(2), Ni(2)−N(4) 2.260(3), Ni(2)−N(5) 2.161(3), Ni(2)−N(6) 2.226(3), Ni(2)−S(1) 2.4395(11), Ni(2)−S(2) 2.5276(15), P−O(1) 1.472(2), P−O(2) 1.482(2); Ni(1)−S(1)−Ni(2) 94.99(4), Ni(1)−S(2)−Ni(2) 90.99(5), O(1)−P−O(2) 120.81(14).

of the $[Ni_2L(\mu\text{-}O_2PH_2)]^+$ cation. Selected bond lengths and angles are given in the figure caption. The hypophosphito ligand bridges the two six-coordinate Ni^{II} atoms in a symmetric fashion, at a Ni···Ni distance of 3.600(1) Å. This distance is a typical value for $[Ni_2L(L')]^{n+}$ complexes coligated with tetrahedral oxoanions.[13] The coordination environment of the nickel atoms is distorted octahedral, as manifested by large deviations from the ideal bond angles. The maximum deviation from the ideal angles is as large as 17.7(1)° (observed for the O(2)−Ni(2)−N(5) angle). The average Ni−N and Ni−S bond distances are 2.270(3) and 2.483(1) Å, respectively. Such bond

lengths are common for bioctahedral Ni(II) complexes supported by L^{2-}.[52,53] The average Ni−O bond lengths at 2.030(2) Å are slightly longer than in the dihydrogenphosphato-bridged $[Ni_2L(\mu\text{-}O_2P(OH)_2)]^+$ complex indicating that hypophosphite binds less strongly to the dinuclear $[Ni_2L]^{2+}$ fragment than dihydrogenphosphate,[12] a fact that is also indicated by a smaller Δ_o value for the hypophosphito complex.

Reactivity of 2. *Exchange of Coligands.* In a recent ligand exchange study we have shown that the stability of $[Ni_2L\text{-}(carboxylato)]^+$ complexes increases with the basicity of the carboxylato ligand.[49] In other words, a more basic carboxylate ligand will replace a less basic one. To examine whether this holds for the hypophosphito complex as well, we performed ligand exchange experiments of 2 with sodium acetate and benzoate.

In an orienting experiment, a reaction of 2 (carrying the weakly basic $H_2PO_2^-$ ion, $pK_b = 12.77$) with sodium acetate ($pK_b = 4.75$) was followed by UV−vis spectroscopy. The results of this titration experiment are shown in Figure 5. Upon addition of increasing amounts of sodium acetate to a solution of 2 a steady shift of the $^3A_{2g} \rightarrow {}^3T_{1g}$ transition band from 671 to 651 nm is observed. Adding further aliquots of NaOAc does not produce further changes. The absorption at 651 nm can be attributed to the presence of the acetate-bridged complex $[Ni_2L(\mu\text{-}O_2CMe)]ClO_4$ (4) which has been reported previously.[20,54]

Having established that the $H_2PO_2^-$ is readily replaced by sodium acetate, we performed the same reaction on a preparative scale. Indeed, when 2 is allowed to react with a slight excess of sodium acetate in methanol a smooth and quantitative exchange of the $H_2PO_2^-$ ion for $CH_3CO_2^-$ takes place (see Scheme 1), and the known carboxylato complex $[Ni_2L(\mu\text{-}O_2CMe)]ClO_4$ (4)[12] (identified by IR spectroscopy and ESI mass spectrometry, Table 2) can be isolated in almost quantitative yield. The same is true for a reaction of 2 with sodium benzoate ($pK_b = 4.25$) which provides $[Ni_2L(\mu\text{-}O_2CPh)]ClO_4$ (5)[55] in very good yield. This clearly shows that the hypophosphito complex 2 is less stable than the carboxylato complexes 4 and 5.

Oxygenation Reactions. Given that hypophosphite is readily oxygenated, we sought to transform 2 with H_2O_2 into a phosphito or phosphato bridged complex. Treatment of hypophosphito complex 2 with H_2O_2 in methanol provides a
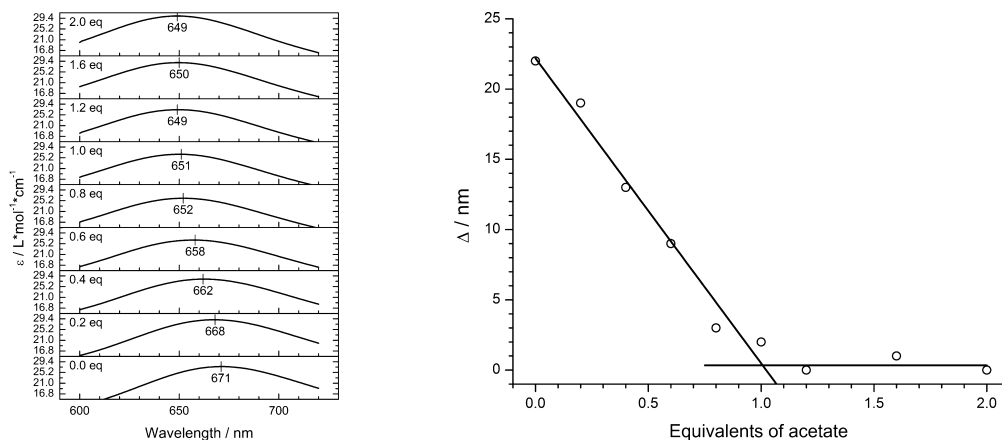

Figure 5. Left: Titration of a 10^{-3} M solution of 2 in acetonitrile/methanol (4:1) with a 10^{-3} M solution of sodium acetate in MeOH monitored by UV−vis spectroscopy (590−730 nm region). Right: Plot of the relative shift of the ν_2 transition of compound 2 (scaled to a final value of 649 nm for the acetate-bridged complex 4) versus added equivalents of sodium acetate, with experimental data shown as open circles.

Table 2. Selected IR [cm⁻¹] and UV−Vis Data [nm] for 4, 5, and 6[a]

assign	$\nu_s(PH_2)$	$\nu_{as}(PH_2)$	$\nu_{as}(PO_2)$	$\nu_s(PO_2)$	$\nu_{as}(RCO_2^-)$	$\nu_s(RCO_2^-)$	$\nu(RSO_3^-)$	ν_1	ν_2	ν_3
4					1589 s	1427 m		650	1131	b
5					1569 s	1406 m		651	1123	b
6	2338 m	2313 m	1168 m	1032 m			1237 s	690	1174	460

[a] m = medium, s = strong, br = broad. [b] ν_3 obscured by strong thiolate→Ni²⁺ charge transfer transitions.

color change from bright green to pale-green. However, instead of the anticipated phosphito or phosphate bridged complex, another hypophosphito complex $[Ni_2L'(\mu\text{-}O_2PH_2)]ClO_4$ (**6**) supported by the hexaamine-diphenylsulfonato ligand $(L')^{2-}$ readily identified by UV−vis spectroscopy (by the lack of intense thiolate→Ni²⁺ transitions) and IR spectroscopy (by IR bands for the RSO_3^- and the $H_2PO_2^-$ ion) has formed (see Table 2). Thus, instead of an oxygenation of the hypophosphito coligand, an S-oxygenation of the supporting N_6S_2 ligand to the known $N_6(SO_3)_2$ (hexaamine-diphenylsulfonato) ligand $(L')^{2-}$ has taken place.[56] The same compound **6** can also be synthesized by using metachloroperbenzoic acid (MCPBA) as an oxidant.[57] The apparent resistance of the $H_2PO_2^-$ ion toward oxidation is attributed to its steric protection by the binding pocket of the $[Ni_2L]^{2+}$ fragment.

Magnetic Properties. Figure 6 displays the temperature dependence of the molar magnetic susceptibility (per dinuclear
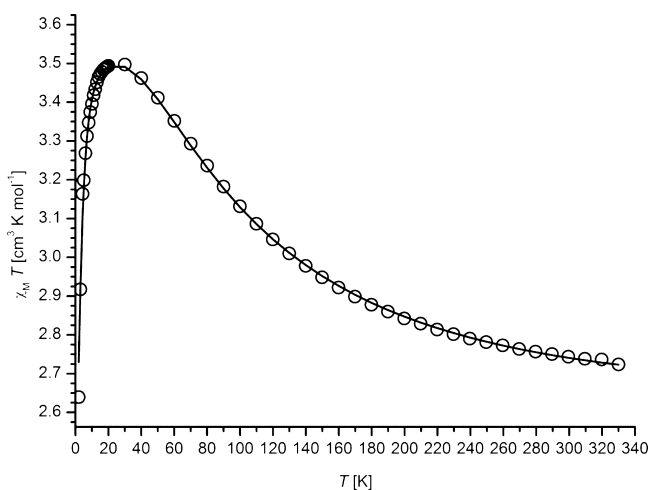

Figure 6. Temperature dependence of $\chi_M T$ for **3** (per dinuclear complex). The full line represents the best theoretical fit to eq 3. Experimental and calculated values are provided as Supporting Information.

complex), in the form of a $\chi_M T$ versus T plot for **3**. The value of $\chi_M T$ increases from 2.72 cm³ K mol⁻¹ (4.67 μ_B) at 330 K to a maximum value of 3.50 cm³ K mol⁻¹ (5.29 μ_B) at 30 K, and then decreases to 2.64 cm³ K mol⁻¹ (4.59 μ_B) at 2 K. This behavior indicates an intramolecular ferromagnetic exchange interaction between the two Ni^II ions that leads to an $S = 2$ ground state of the hypophosphito complex. The decrease in $\chi_M T$ below 20 K can be attributed to zero-field splitting of Ni^II and/or saturation effects.

The temperature dependence of the magnetic data of complex **3** was simulated using the appropriate spin-Hamiltonian (eq 3)[58] which contains a Zeeman and a zero-field splitting term applying a full-matrix diagonalization approach.[59] The introduction of a D parameter is appropriate for octahedral Ni^II, since the noncubic components of the

ligand field may act on the ³A₂g ground state to produce a zero-field splitting which may be of the same order of magnitude as J.[60,61] The values of g and D were assumed to be identical for both nickel ions.

$$H = -2JS_1S_2 + \sum_{i=1}^{2}[D_i(\hat{S}_{iz}^2 - 1/3S_i(S_i + 1)) + g_i\mu_B B_\tau \hat{S}_{i\tau}]$$

$$(t = x, y, z) \tag{3}$$

By taking into account the zero-field splitting and temperature independent paramagnetism,[62] a good fit of the experimental data, shown in Figure 6 as a solid line, was possible over the full temperature range, yielding $J = +22$ cm⁻¹, $g = 2.17$, TIP = 1.40×10^{-4} cm³ mol⁻¹, and $D = -8.12$ cm⁻¹. However, the value of the zero-field splitting parameter should be taken as indicative rather than definite, because temperature dependent magnetic susceptibility measurements are not very appropriate for the determination of D.[63,64] This is corroborated by a two-dimensional projection of the relative error surface for varying J and D (Figure S1). Instead of one global minimum the error surface exhibits two minima with the same relative error corresponding to the combinations $D = -8.12$ cm⁻¹, $J = +22$ cm⁻¹ and $D = +8.12$ cm⁻¹, $J = +22$ cm⁻¹.[65] Nevertheless, J is not influenced markedly by the value of D and represents an accurate measure of the magnetic coupling in this complex. The $S = 2$ ground state for **3** is confirmed by field dependent magnetization measurements (see Supporting Information).

It has been noted previously that there exists a relationship between the sign and magnitude of the coupling parameter and the Ni−S−Ni angle in bioctahedral dinickel(II) complexes supported by L^{2-}.[53,66] The coupling is antiferromagnetic in nature if the Ni−S−Ni angle deviates by more than ≈ ± 10° from 90°. For angles within the 90 ± 10° range a ferromagnetic interaction is observed. The observation of a ferromagnetic exchange interaction in **3**, for which the average Ni−S−Ni angles is in the 90 ± 10° range, is in good agreement with the reported trend.

In complex **3** two coupling pathways are possible, one through the thiolato and one through the hypophosphito coligand. In order to establish the predominant coupling path, we have compared some $[Ni_2L(L')]^+$ complexes with an $S = 2$ ground state. Table 3 lists the J and g values of the selected examples, along with their Ni···Ni distances and Ni−S−Ni angles. As can be seen, the Ni···Ni distances and the Ni−S−Ni angles lie within very narrow ranges, and the same holds for the J values as well. The similar J values imply that the magnetic exchange interactions are predominantly propagated via the two thiophenolato bridges (in case that the Ni−S−Ni angles are close to 90°). In view of longer coupling pathways through the Ni−L′−Ni bridges, this is not surprising.

DFT Calculations. We performed DFT calculations to get more insights into the magnetic coupling in the $[Ni_2L(\mu\text{-}O_2PH_2)]^+$ complex. With regards to the type of the exchange interaction, our calculations predict a ferromagnetic coupling in

Table 3. Magnetic Properties and Metrical Data of Selected $[Ni_2L(L')]^+$ Complexes Supported by the N_6S_2 Macrocycle L^{2-}

complex	J^a [cm^{-1}]	g	Ni···Ni [Å]	Ni−S−Ni [deg]	ref
$[Ni_2L(\mu\text{-}O_2PH_2)]^+$ (3)	+22.0	2.17	3.600(1)	93.00(4)	this work
$[Ni_2L(\mu\text{-}OAc)]^+$ (4)	+21.7	2.14	3.483(1)	89.65(4)	55
$[Ni_2L(\mu\text{-}OBz)]^+$ (5)	+18.4	2.19	3.491(1)	89.56(4)	55
$[Ni_2L(\mu\text{-}H_2BH_2)]^+$	+27.0	2.09	3.458(1)	89.87(4)	67
$[Ni_2L(\mu_{2,3}\text{-}N_4CCH_3)]^{+b}$	+20.0	2.20	3.425(1)	87.12(3)	68

[a] Parameters resultant from least-squares fit to the $\chi_M T$ data under the spin Hamiltonian in [eq 3], J = coupling constant ($\mathbf{H} = -2J\mathbf{S}_1\mathbf{S}_2$), g = g-value. [b] $N_4CCH_3^-$ = 5-methyl-tetrazolato.

agreement with the experimental data and regardless of the applied exchange correlation functional. However, the DFT-(PBE) calculation (J = 38 cm^{-1}) overestimates the exchange coupling, an effect which is well-known since standard DFT exchange correlation functionals do not localize the d-states sufficiently.[69,70] The B3LYP density functional somewhat corrects for this DFT failure by mixing Hartree−Fock exact exchange into the functional. Therefore, the exchange coupling evaluated from the B3LYP calculations is often in better agreement with the experimental ones.[71] Accordingly, the calculated B3LYP exchange interaction (J = 16 cm^{-1}) is closer to the experimental one.

To gain a more detailed insight into the magnetic coupling an additional DFT(PBE) calculation without the bridging hypophosphito ligand was performed. The overall ferromagnetic coupling is preserved upon this removal; however, the strength of the coupling is reduced by a factor of 2 resulting in J = 15 cm^{-1}. The lowering of the J value indicates that the $H_2PO_2^-$ ion provides a coupling path and contributes to the ferromagnetic exchange coupling. Figure S3a shows a perspective view of a molecular orbital presenting a distinctive pathway across the $H_2PO_2^-$ ion in 3. According to the Anderson−Goodenough−Kanamori rules[72−75] another ferromagnetic coupling path via the sulfur atoms should be available since the Ni−S−Ni angles in 3 are close to 90° (Ni1−S1−Ni2 94.99(4)°, Ni1−S2−Ni2 90.99(5)°). Indeed, such a pathway across the sulfur atoms is available as indicated by Figure S3b. This result is in good agreement with the reported trend.[53]

Another, more quantitative, point of view is based on the Hay−Thibeault−Hoffmann model,[76] where the square of the energy difference $(\Delta e)^2$ of the unoccupied magnetic orbitals at the metal centers is of interest. In the case of 3 we are confronted with a very small energy difference of $(\Delta e)^2$ = 0.0173 eV^2 of the unoccupied Ni orbitals. This value lies within the range of $(\Delta e)^2$ = 0.0−0.027 eV^2 typical for $[Ni_2L(L')]^+$ complexes for which a ferromagnetic exchange interaction is expected.[53]

Figure S4 shows the density of states close to the Fermi Level E_F, which is defined in the middle of the HOMO−LUMO gap (E_F = (LUMO−HOMO)/2). One can immediately see that the HOMO can be attributed to majority spins while the LUMO consists of minority spins. The HOMO−LUMO gap (HLG) between these two states is 1.27 eV. The HLG for majority spins is considerably larger (2.82 eV), and the HLG for minority spins (1.82 eV) is in between the majority HLG and

the overall HLG. In essence all states close to E_F are dominated by Ni d-states. This would also be in good qualitative agreement with the cyclic voltammetry experiments described above where the first oxidation of $[Ni_2L(\mu\text{-}O_2PH_2)]^+$ is metal-centered (Ni^{2+} → Ni^{3+}) in nature.

CONCLUDING REMARKS

The main findings of the present work can be summarized as follows: (i) The dinuclear hypophosphito-bridged Ni(II) complex $[Ni_2L(\mu\text{-}O_2PH_2)]^+$ supported by a macrocyclic hexamine-dithiophenolate ligand is readily prepared, and can be isolated as an air-stable perchlorate $[Ni_2L(\mu\text{-}O_2PH_2)]ClO_4$ (2) or tetraphenylborate $[Ni_2L(\mu\text{-}O_2PH_2)]BPh_4$ (3) salt. (ii) Complex salts 2 and 3 were found to be thermally stable both in solution as well as in the solid state, which contrasts the behavior of other nickel hypophosphito systems, which are readily reduced by hypophosphite. (iii) The stabilization is believed to be a consequence of the steric protection offered by the supporting macrocycle. (iv) The bisoctahedral $[Ni_2L(\mu\text{-}O_2PH_2)]^+$ cation has a $N_3Ni(\mu_{1,3}\text{-}O_2PH_2)(\mu\text{-}S)_2NiN_3$ core structure with the hypophosphito ligand attached to the two Ni^{II} ions in a $\mu_{1,3}$-bridging mode. (v) The hypophosphito ligand can be replaced by carboxylates, in agreement with a higher affinity of the $[Ni_2L]^{2+}$ dication for more basic oxoanions. (vi) Treatment of $[Ni_2L(\mu\text{-}O_2PH_2)]ClO_4$ with H_2O_2 or MCPBA results in the oxidation of the bridging thiolato to sulfonato groups. The hypophosphito group is not oxidized under these conditions again most likely due to the steric protection offered by the supporting N_6S_2 macrocycle. (vii) The $O_2PH_2^-$ unit in 2 is redox inactive in a potential window from −2.0 to +2.5 V versus SCE. (viii) Finally, the spins of the nickel(II) (S_i = 1 ions) in 3 are weakly ferromagnetically coupled [J = 23 cm^{-1}, ($\mathbf{H} = -2J\mathbf{S}_1\mathbf{S}_2$)] to produce an S = 2 ground state.

ASSOCIATED CONTENT

Ⓢ Supporting Information

X-ray crystallographic data of 3•MeCN in CIF format. Experimental and calculated susceptibility data, experimental and calculated magnetization data and DFT calculation for 3. This material is available free of charge via the Internet at http://pubs.acs.org.

AUTHOR INFORMATION

Corresponding Author
*E-mail: b.kersting@uni-leipzig.de. Fax: +49/(0)341-97-36199.

Present Address
§Institute of Chemistry, Academy of Sciences of Moldova Academiei str. 3, MD-2028, Chisinau, Republic of Moldova.

Notes
The authors declare no competing financial interest.

ACKNOWLEDGMENTS

REFERENCES

(1) Marcos, M. D.; Ibanez, R.; Amoros, P.; LeBail, A. *Acta Crystallogr.* 1991, *47C*, 1152−1155.

(2) Weakley, T. J. R. *Acta Crystallogr.* **1979**, *35B*, 42−45.

(3) Marcos, M. D.; Amoros, P.; Sapina, F.; Beltran-Porter, A.; Martinez-Manez, R.; Attfield, J. P. *Inorg. Chem.* **1993**, *32*, 5044−5052.

(4) Matsuzaki, T.; Itaka, Y. *Acta Crystallogr.* **1969**, *25B*, 1932−1938.

(5) Weakley, T. J. R.; Watt, W. W. L. *Acta Crystallogr.* **1979**, *35B*, 3023−3024.

(6) Seddon, J. A.; Jackson, A. R. W.; Kresiński, R. A.; Platt, A. W. G. *Polyhedron* **1996**, *15*, 1899−1902.

(7) Seddon, J. A.; Jackson, A. R. W.; Kresiński, R. A.; Platt, A. G. W. *J. Chem. Soc., Dalton Trans.* **1999**, 2189−2196.

(8) Tanner, P. A.; Hung, S.-T.; Mak, T. C. W.; Ru-Ji, W. *Polyhedron* **1992**, *11*, 817−822.

(9) Johnson, N. C.; Bull, W. F. *Inorg. Chim. Acta* **1978**, *27*, 191−195.

(10) Linn, D. E.; Gould, E. S. *Inorg. Chem.* **1987**, *26*, 3442−3446.

(11) Baran, E. J.; Etchevery, S. B.; Diemann, E. *Polyhedron* **1985**, *4*, 1711−1715.

(12) Kersting, B. *Angew. Chem.* **2001**, *113*, 4109−4112; *Angew. Chem., Int. Ed.* **2001**, *40*, 3987−3990.

(13) Lozan, V.; Kersting, B. *Eur. J. Inorg. Chem.* **2007**, 1436−1443.

(14) Lozan, V.; Kersting, B. *Inorg. Chem.* **2006**, *45*, 5630−5634.

(15) Steinfeld, G.; Kersting, B. *Z. Anorg. Allg. Chem.* **2009**, *635*, 260−264.

(16) Lozan, V.; Lach, J.; Kersting, B. *Inorg. Chem.* **2012**, *51*, 5213−5223.

(17) Scholder, H.; Heckel, H. *Z. Anorg. Allg. Chem.* **1931**, *198*, 329−351.

(18) Riedel, W. In *Electroless Nickel Plating*; ASM: Metals Park, OH, 1991; pp 11−32.

(19) Under our experimental conditions $E(Cp_2Co^+/Cp_2Co) = -1.345$ V vs $E(Cp_2Fe^+/Cp_2Fe)$; $E(Cp_2Co^+/Cp_2Co) = -0.937$ V vs SCE. Connelly, N. G.; Geiger, W. E. *Chem. Rev.* **1996**, *96*, 877−910.

(20) Hausmann, J.; Klingele, M.-H.; Lozan, V.; Steinfeld, G.; Siebert, D.; Journaux, Y.; Girerd, J.-J.; Kersting, B. *Chem.—Eur. J.* **2004**, *10*, 1716−1728.

(21) *SMART, Data Collection Program for the CCD Area-Detector System*; Bruker Analytical X-ray Systems: Madison, WI, 1997.

(22) *SAINT+, V6.02, Data Reduction and Frame Integration Program for the CCD Area-Detector System*; Bruker AXS: Madison, WI, 1999.

(23) Sheldrick, G. M. *Program SADABS: Area-Detector Absorption Correction*; University of Göttingen: Göttingen, Germany, 1996.

(24) Sheldrick, G. M. *Acta Crystallogr.* **1990**, *A46*, 467−473.

(25) Sheldrick, G. M. *SHELXTL NT 5.10*; Bruker AXS: Bruker AXS, Madison, WI, 1998.

(26) (a) Farrugia, L. J. *ORTEP 3 for Windows, Version 1.05*; University of Glasgow: Glasgow, U.K., 1997. (b) Farrugia, L. J. *J. Appl. Crystallogr.* **1997**, *30*, 565.

(27) Briley, A.; Pederson, M.; Jackson, K.; Patton, D.; Porezag, D. C. *Phys. Rev. B.* **1998**, *58*, 1786−1793.

(28) Jackson, K.; Pederson, M. *Phys. Rev. B.* **1990**, *42*, 3276−3281.

(29) Pederson, M.; Jackson, K. *Phys. Rev. B.* **1990**, *41*, 7453−7461.

(30) Pederson, M.; Jackson, K. *Phys. Rev. B.* **1991**, *43*, 2840−2847.

(31) Pederson, M.; Porezag, D.; Kortus, J.; Patton, D. *Phys. Status Solidi B* **2000**, *217*, 197−218.

(32) Porezag, D.; Pederson, M. *Phys. Rev. B* **1996**, *54*, 7830−7836.

(33) Quong, A.; Pederson, M.; Feldman, J. *Solid State Commun.* **1993**, *87*, 535−539.

(34) Porezag, D.; Pederson, M. *Phys. Rev. A.* **1999**, *60*, 2840−2847.

(35) Perdew, J.; Burke, K.; Ernzerhof, M. *Phys. Rev. Lett.* **1996**, *77*, 3865−3868.

(36) Perdew, J.; Burke, K.; Ernzerhof, M. *Phys. Rev. Lett.* **1997**, *78*, 1396−1396.

(37) Neese, F. *J. Chem. Phys.* **2003**, *119*, 9428−9444.

(38) Neese, F. *Int. J. Quantum Chem.* **2001**, *83*, 104−114.

(39) Becke, A. D. *J. Chem. Phys.* **1993**, *98*, 5648−5653.

(40) Schaefer, A.; Horn, H.; Ahlrichs, R. *J. Chem. Phys.* **1992**, *97*, 2571−2577.

(41) Loose, C.; Ruiz, E.; Kersting, B.; Kortus, J. *Chem. Phys. Lett.* **2008**, *452*, 38−43.

(42) Yoshizawa, M.; Kusakawa, T.; Fujita, M.; Yamaguchi, K. *J. Am. Chem. Soc.* **2000**, *122*, 6311−6312.

(43) Schaible, B.; Roessel, K.; Weidlein, J.; Hausen, H. D. *Z. Anorg. Allg. Chem.* **1974**, *409*, 176−184.

(44) Nakamoto, K. *Infrared and Raman Spectra of Inorganic and Coordination Compounds*, 5th ed.; VCH-Wiley: New-York, 1997.

(45) Bickley, R. I.; Edwards, H. G. M.; Gustar, R. E.; Tait, J. K. F. *J. Mol. Struct.* **1992**, *273*, 61−72.

(46) McAuley, A.; Subramanian, S. *Inorg. Chem.* **1990**, *29*, 2830−2837.

(47) Adam, K. R.; Antolovich, M.; Baldwin, D. S.; Bridgen, L. G.; Duckworth, P. A.; Lindoy, L. F.; Bashall, A.; McPartlin, M.; Tasker, P. A. *J. Chem. Soc., Dalton Trans.* **1992**, 1869−1876.

(48) Lever, A. B. P. *Inorganic Electron Spectroscopy*, 2nd ed.; Elsevier Science: Amsterdam, 1984.

(49) Lehmann, U.; Klingele, J.; Lozan, V.; Steinfeld, G.; Klingele, M. H.; Käss, S.; Rodenstein, A.; Kersting, B. *Inorg. Chem.* **2010**, *49*, 11018−11029.

(50) The UV−vis spectrum of 2^{2+} [$\lambda_{max} = 400$ ($\varepsilon_{max} = 4368$ M^{-1} cm^{-1}), 506 (4283 M^{-1} cm^{-1}), 777 nm (7320 M^{-1} cm^{-1})] reveals several strong absorptions attributable to ligand-to-metal (RS$^-$→Ni^{III}) charge-transfer transitions. There is also a feature at 1346 nm (2538 M^{-1} cm^{-1}) attributable to an intervalence transition. Electrospray ionization mass spectrometry (ESI(+)-MS): m/z (CH$_3$CN) = 950.26 [Ni^{II}Ni^{III}L(μ-O$_2$PH$_2$)]ClO$_4^+$, 424.66 [Ni^{II}Ni^{III}L(μ-O$_2$PH$_2$)]$^{2+}$. So far, all attempts to isolate the [Ni$_2$L(μ-O$_2$PH$_2$)]$^{2+}$ dication have been unsuccessful.

(51) Journaux, Y.; Glaser, T.; Steinfeld, G.; Lozan, V.; Kersting, B. *Dalton Trans.* **2006**, 1738−1748.

(52) Kersting, B. *Z. Anorg. Allg. Chem.* **2004**, *630*, 765−780.

(53) Lozan, V.; Loose, C.; Kortus, J.; Kersting, B. *Coord. Chem. Rev.* **2009**, *253*, 2244−2260.

(54) Lozan, V.; Holldorf, J.; Kersting, B. *Inorg. Chim. Acta* **2009**, *362*, 793−798.

(55) Lach, J.; Hahn, T.; Kersting, B.; Kortus, J. *Eur. J. Inorg. Chem.* **2012**, 2381−2388.

(56) Käss, S.; Kersting, B. *Eur. J. Inorg. Chem.* **2012**, 2389−2401.

(57) Dinuclear nickel(II) complexes supported by the hexamine-disulfonate ligand (L′)$^{2-}$ are more inert to substitution than those supported by the hexaaza-dithiophenolate (L)$^{2-}$ ligand. This explains why the H$_2$PO$_4^-$ ion in **6** is not exchanged for the *meta*-chlorobenzoate ions (present in the reaction medium), see: Hausmann, J.; Käss, S.; Kersting, B.; Klod, S.; Kleinpeter, E. *Eur. J. Inorg. Chem.* **2004**, 4402−4411.

(58) Kahn, O. *Molecular Magnetism*; VCH-Wiley: New York, 1993.

(59) Azuah, R. T.; Kneller, L. R.; Qiu, Y.; Tregenna-Piggott, P. L. W.; Brown, C. M.; Copley, J. R. D.; Dimeo, R. M. *J. Res. Natl. Inst. Stand. Technol.* **2009**, *114*, 341−358.

(60) Boča, R.; Dlháň, L.; Haase, W.; Herchel, R.; Mašlejová, A.; Papánková, B. *Chem. Phys. Lett.* **2003**, *373*, 402−410.

(61) Mukherjee, P.; Drew, M. G.; Tangoulis, V.; Estrader, M.; Diaz, C.; Ghosh, A. *Polyhedron* **2009**, *28*, 2989−2996.

(62) Carlin, R. L. *Magnetochemistry*; Springer, Berlin, 1986; pp 12−13.

(63) Ginsberg, A. P.; Martin, R. L.; Brookes, R. W.; Sherwood, R. C. *Inorg. Chem.* **1972**, *11*, 2884−2889.

(64) Nanda, K. K.; Addison, A. W.; Paterson, N.; Sinn, E.; Thompson, L. K.; Sakaguchi, U. *Inorg. Chem.* **1998**, *37*, 1028−1036.

(65) Bill, E. *julX*; http://ewww.mpi-muelheim.mpg.de/bac/logins/bill/julX_en.php.

(66) Krupskaya, Y.; Alfonsov, A.; Parameswaran, A.; Kataev, V.; Klingeler, R.; Steinfeld, G.; Beyer, N.; Gressenbuch, M.; Kersting, B.; Büchner, B. *ChemPhysChem* **2010**, *11*, 1961−1970.

(67) Journaux, Y.; Lozan, V.; Hausmann, J.; Kersting, B. *Chem. Commun.* **2006**, 83−84.

(68) Lach, J.; Voitekhovich, S. V.; Lozan, V.; Gaponik, P. N.; Ivashkevich, O. A.; Lincke, J.; Lässig, D.; Kersting, B. *Z. Anorg. Allg. Chem.* **2010**, *636*, 1980−1986.

(69) Gunnnarsson, O.; Lundqvist, B. I. *Phys. Rev. B* **1976**, *13*, 4274−4280.

(70) Kortus, J.; Hellberg, C. S.; Pederson, M. R. *Phys. Rev. Lett.* **2001**, *86*, 340−3403.

(71) Ruiz, E.; Alemany, P.; Alvarez, S.; Cano, J. *J. Am. Chem. Soc.* **1997**, *119*, 1297−1303.

(72) Anderson, P. W. Theory of Magnetic Exchange Interactions: Exchange in Insulators and Semiconductors, Advances in Research and Applications. In *Solid State Physics*; Seitz, F., Turnbull, D., Eds.; Academic Press, New York, 1963; Vol. *14*, p 99.

(73) Goodenough, J. B. *Phys. Rev. B.* **1955**, *100*, 564−573.

(74) Goodenough, J. B. *Phys. Chem. Solids* **1958**, *6*, 287−297.

(75) Kanamori, J. *Phys. Chem. Solids* **1959**, *10*, 87−98.

(76) Hay, P. J.; Thibeault, J. C.; Hoffmann, R. *J. Am. Chem. Soc.* **1975**, *97*, 4884−4899.